FINAL REPORT ON INTERAGENCY AGREEMENT BETWEEN THE RADAR OPERATIONS CENTER AND THE OFFICE OF HYDROLOGIC DEVELOPMENT
Covering the period 1 April 2009 to March 31 2010

Dennis Miller, David Kitzmiller, Shaorong Wu

Executive Summary

Task 1. Investigate the effectiveness of rainfall estimation methods in conditions of partial beam blockage

A study of the use of power-enhanced Zh and Kdp in sectors with known terrain beam blockage was completed. It appears that the method of enhancing returned power in the horizontally-polarized beam is effective in blockage up to 90%. The method for applying R(Kdp) in zones of partial beam blockage appears to have little additional skill. We suggest some further studies to determine the effectiveness of enhancing returned power in sectors with blockage > 50%, rather than using a higher antenna elevation, as is the current default practice.

Task 2. Collection of surface snowfall estimates for use in validation and calibration of dual polarimetric radar-based snowfall algorithms

As noted in the last report, datasets for the 2007-2008 winter season in the area of northern Indiana and Illinois were collected from ASOS and CoCoRAHs reports. Digital data were forwarded to ROC and NSSL staff. The overall project of dual-polarization snowfall algorithm development has since been put on hiatus. However we can collect more data from these sources when necessary.

Task 3. Investigation modification of MPE bias table to apply to dual pol quantitative precipitation estimates (QPE)

A research plan has been drafted and discussed with the ROC POC. We propose to investigate mean-field bias, range-dependent bias, and local bias corrections. An extensive dataset of gauge-radar QPE pairs from the legacy Precipitation Processing System has been collected. An initial analysis of this data shows some operationally-appreciable differences between the proposed methods, depending on precipitation climatology and density of the rain gauge network. Collection of dual-polarization QPE products from the pre-production KOUN unit, and collocated 1-hour rain gauge reports from Oklahoma networks, has been initiated by the OHD Hydrologic Software Engineering Branch. Tests of bias correction on this data will be initiated when all parties agree that data quality meets expected operational standards.

Task 1. Investigate effectiveness of rainfall estimation methods in conditions of partial beam blockage

1. INTRODUCTION

The NOAA National Weather Service (NWS) is continually endeavoring to improve the hydrometeorological products it uses in operations and provides to the public. Among these are quantitative precipitation estimates (QPE), which are crucial to NWS's hydrologic prediction on timescales ranging from hourly to 6-hourly to daily, and spatial scales ranging from local to regional to national. A principal component of these QPE fields is the estimates provided by radar. Operationally, these are collected from a national network of more than 120 S-band (~10 cm wavelength) "Weather Service Radar-1988 Doppler" (WSR-88D) radars. Because of its potential to resolve precipitation at small time and space scales, radar QPE is especially important in hydrologic prediction for small basins prone to flash flooding, and in complex terrain (Smith et al. 2000; Filiaggi et al. 2002; Smith et al. 2004b).

In the WSR-88D, QPE is determined via temporal integration of instantaneous precipitation rates (R; mm/hr) generally sampled about once every five minutes. Presently, R is derived from the single-polarized, base reflectivity field (Z; mm^6/m^3); however, the NWS is in the process of upgrading the WSR-88D from a single polarization to a dual polarization system (Ryzhkov et al. 2005a). Once this upgrade is complete and validated, R will be determined from several dual polarization moments including differential reflectivity (Zdr) and specific differential phase (Kdp), as well as the traditional Z. Which of these estimators, or combinations thereof, is used when and where is determined by a classification of the type of precipitation (e.g. light rain; heavy rain; hail; graupel; snow; etc.) occurring at any given time and location (Ryzhkov et al. 2005b; Park et al. 2009).

Where the radar signal is unblocked by terrain or other obstacles or is not filtered or significantly refracted by atmospheric conditions, each WSR-88D unit can provide precipitation estimates to a nominal range of 230 km. In the methodology of the WSR-88D "Hybrid Scan" (Fulton et al. 1998), in azimuth sectors where the radar beam is deemed "fully blocked" (in operational practice, where the blockage exceeds a threshold, usually 50%), the next-higher elevation that is not fully blocked is utilized as the basis of the precipitation rate estimate. The elevation that is finally selected may be partially blocked. In such cases, the determination of which radar moment should be used would be dependent upon the behavior of that moment in the presence of beam blockage, as well as on the predominant hydrometeor type. Estimates that are based upon reflectivity-power, such as Z and Zdr, are known to be diminished in the presence of blockage, while estimates based upon differential phase (Φdp), such as Kdp, are believed to be unaffected by such blockage, unless nearly complete (Brandes 2000)

At the NWS Office of Hydrologic Development (OHD), we have recently concluded a study seeking to improve the NWS operational QPE process in the presence of partial beam blockage, using dual-polarization moments. The fundamental methodology was to

compare four approaches to radar-based precipitation estimation in situations with substantial terrain-induced beam blockage. The first two approaches are based upon the traditional, horizontal polarization-based Z-R relationship, without and with enhancement of the reflectivity-power field (Zenh) to compensate for partial beam blockage. In the enhancement methodology, we attempted to correct outbound and returned power in sectors with blockage up to 90%, under standard refraction conditions. A third approach is based upon the dual-polarization Kdp field that is, theoretically, insensitive to beam blockage. The fourth approach attempts to optimally combine the Zenh and Kdp methodologies in a manner analogous to that planned for use in the target, Dual Polar, WSR-88D precipitation estimation system, in situations where non-nominal beam-blockage is present..

2. BACKROUND and MOTIVATION

A primary motivation for this study is that the WSR-88D system is in the process of being upgraded from single polarization to dual polarization capability. In anticipation, a new, Dual-Polar QPE algorithm has been incorporated into the latest-release WSR-88D code ("Build 12") and is presently being assessed for potential, national, operational implementation. That algorithm, developed by staff of the NOAA/National Severe Storms Laboratory (NSSL), utilizes the Kdp field as the basis for precipitation estimates in situations of non-nominal beam-blockage, at places and times when a preliminary, hydrometeor classification algorithm (Ryzhkov et al. 2005b) had determined the predominant hydrometeor type to be 'heavy rain' or 'rain mixed with hail'. The Kdp moment, which is determined as the first-order spatial derivative in the radial direction of the differential phase field (Φdp), is generally believed to be "insensitive to radar calibration, partial beam blockage, propagation effects, and system noise" (Brandes, 2000; also Freidrich et al. 2007; Lang et al. 2009). Hence, it is expected to remain effective as a precipitation estimator even in the presence of rather substantial beam blockage. Despite this potential advantage over other radar fields commonly used as the basis of QPE estimates, its use in the target, Dual-Polar QPE algorithm is presently limited to those situations where certain hydrometeor types predominate. One goal of our investigation was to assess whether, for an S-band radar in the presence of partial beam blockage, Kdp may have more general advantages as a precipitation estimator for many hydrometeor classes including light/moderate rain.

Furthermore, in the single polarization, R(Z)-based "Precipitation Processing System" (PPS) algorithm (Fulton et al. 1998) that still runs, operationally, in the WSR-88D, reflectivity-power enhancement is applied to compensate for partial beam blockage, but the upper limit of blockage at which that enhancement is applied rarely exceeds a default threshold of 50% (resulting in 2x power enhancement by the PPS method; see equations in section 3d, below). Another aspect of our motivation was to determine whether further enhancement of the horizontally-polarized reflectivity field, in the presence of high but not complete beam blockage, might prove an effective approach to precipitation estimation. We compared the effectiveness of using the basic Z-R relationship to compensate for beam blockage up to 90% (corresponding to 10x power enhancement)

against that of applying R(Kdp) more broadly than to just the usual, heavy rain or rain-mixed-with-hail situations.

3. DATA AND METHODOLOGY

3a. Approach

Our basic approach was to prepare precipitation estimates via various methodologies from base data collected by an S-band, dual polar radar in a mountainous environment, and compare those, visually and statistically, against verification fields prepared from a combination of rain gauge and WSR-88D radar data. We utilized an in-house processing environment that employed the same, core logic to generate the fundamental precipitation estimates as that employed in the new suite of WSR-88D, dual polar-based rainfall estimation algorithms (Ryzhkov et al. 2005a), though our environment did not contain all the detail and complexity of that system – i.e. we did not precede our analysis with a hydrometeor classification determination at all sample bin locations, nor did we process a multi-elevation "hybrid scan"; our assessment was confined to the 0.5 degree elevation angle.

3b. Base radar data

At the time of our study, essentially no WSR-88D dual polar, base data were available from locations with significant terrain height and variability. We located suitable data for our purposes from a field experiment conducted by the NCAR Earth Observing Laboratory (EOL) utilizing its dual polar, S-band unit ("S-Pol") in northeastern Colorado, near Boulder, during June-August 2006 (the Refractivity Experiment for H_2O Research and Collaborative Operational Technology Transfer, or REFRACTT project; Roberts et al. 2008). The coverage umbrella of that radar site featured substantial sectors with partial beam blockage in the south-southeast and north-northwest, as well as broad sectors with little blockage in the east, and ones with almost complete blockage, even at low elevation angles, in the west (see Figure 1a). An important advantage of this siting was the availability of "Stage IV", gridded gauge-radar precipitation estimates across the entire S-Pol umbrella, for use in verification (see section 3e, below). The sectors partially blocked relative to the S-pol unit were fully visible to the WSR-88D units at Denver International Airport (KFTG) or Cheyenne, Wyoming (KCYS). During the 161 hours of data used in our study, the predominant precipitation type was convective, and numerous instances of rainfall coincident with partial beam blockage occurred.

3c. **Beam blockage determination**

In order to determine percent terrain-blockage at individual sample bin locations for this siting, we employed the operational algorithm and digital elevation model used to generate beam blockage maps at WSR-88D sites, applying it, in our case, at the exact az/ran/height of the S-Pol location, east of Boulder. Figure 1b shows beam blockage, by percentage, at 0.5^0 antenna elevation for that location after translation to the 4 km x 4 km,

polar-stereographic, Hydrologic Research and Analysis Projection (HRAP) grid system often used in NWS hydrologic analyses (Fulton et al. 1998, Reed and Maidment 1999).

3d. Radar QPE preparation

We employed the four methodologies mentioned above for preparing QPE estimates, as follows:

a) R(Z) or R(Z0):

We utilized the classic, Z-R relationship for estimating precipitation rate from reflectivity-power, incorporating the multiplicative and power-coefficients employed in the WSR-88D "Convective" relationship, i.e.:

$$R(Z) = (Z/a)^{1/b}$$

where Z is the (horizontally-polarized) reflectivity-power (mm^6/m^3); R is the instantaneous rainfall rate (mm/hr); a, b are the Z-R multiplicative & power coefficients (300.0; 1.4, respectively). We included this methodology in our study primarily to provide a basis for comparison to our R(Z) methodology that compensates for terrain-beam blockages, below.

b) R(Zenh) or R(Z90):

We again employed the classic, Z-R relationship, but this time after the reflectivity-power was enhanced proportionally to compensate for beam-blockage in the manner of the single polar-based WSR-88D PPS, though we corrected to a higher threshold:

$$Blk_Fact = 1.0 / (1.0 - B)$$
$$(B <= B_{threshold})$$

$$Zadj = (10^{dBZ / 10.0}) * Blk_Fact$$

$$R(Zenh) = (Zadj/a)^{1/b}$$

where: B is the fractional beam blockage (to nearest 0.01) at a given sample bin location; $B_{threshold}$ is the upper threshold of beam blockage for which a correction is applied (i.e. 0.90); Blk_Fact is the blockage factor by which a bin's reflectivity power is enhanced; Zadj is the blockage-adjusted reflectivity power (mm^6/m^3); dBZ is the base reflectivity in decibel (log10) units; R(Zenh) is the enhanced rainfall rate after compensation for blockage (mm/hr); and a, b are the multiplicative & power coefficients of the Z-R relationship (as above)

To determine B on a bin-by-bin basis, we utilized the same methodology as used to determine blockage configuration files at operational WSR-88D sites, but applied, at the lat/lon/height of the S-Pol radar. Each bin's reflectivity-power is enhanced

proportionally to B, though we cap B at 0.9 (bins with greater than 90% blockage were not included in our analysis.) At the 0.9 threshold, the reflectivity power enhancement is equal to 10. Note that this methodology is very similar to that intended for use under terrain-blocked conditions in the targeted, WSR-88D Dual-Polar QPE algorithm, in situations where the hydrometeor type is *not* heavy rain or rain-hail mix.

c) R(n-Kdp):

We utilized a rainfall estimation methodology based primarily on the specific differential phase field, Kdp, as described in the WSR-88D Dual Polarization Preprocessor and QPE algorithm documentation (Ryzhkov et al. 2005a). This version determines rainfall rates from Kdp unless that field is negative, which we found to occur in 0.03% to 2.0 % of sample bins during any individual hour in our study. In the final operational version of the algorithm, such rainrates are replaced by the R(Z) estimate (Daniel Stein, James Ward, personal communication). For instances with Kdp < 0, we substituted a rainfall rate based upon the horizontally-polarized reflectivity field, i.e.:

$R(Kdp) = ak * |Kdp|^{bk} * sign(Kdp)$

IF R(Kdp) >= 0
THEN
    R(n-Kdp) = R(Kdp)
ELSE
    $R(n\text{-}Kdp) = R(Zenh) = (Zadj/a)^{1/b}$
ENDIF

where R(Kdp) is the instantaneous rainfall rate (mm/hr) dependent only upon the Kdp field; ak is the multiplicative coefficient of the R(Kdp) relationship (44.0); bk is the power coefficient of the R(Kdp) relationship (0.822); and sign(Kdp) indicates that the rainfall rate maintains the same mathematical sign (+/-) as Kdp. This methodology is included in our study to assess whether Kdp may have more general benefits as a precipitation estimator – particularly under conditions of significant beam blockage – than in just the heavy rain or rain-hail mix situations to which its use is normally restricted.

d) R(Kdp-h):

Here we employed a hybrid version of precipitation estimation combining the R(n-Kdp) methodology of our part c, above, for heavier precipitation rates, with the R(Zenh) methodology of our part b, for lighter precipitation rates. To distinguish between the lighter and heavier rates, we employed a threshold (same as used in the WSR-88D Dual Polar QPE algorithm) below which R(Kdp) has been shown in preliminary experiments to be less effective as a precipitation estimator, i.e.:

IF R(Kdp) < 0 OR R(Zenh) < 10 mm h^{-1}

THEN
    R(Kdp-h) = R(Zenh)
ELSE
    R(Kdp-h) = R(Kdp)
ENDIF

where 10 mm h^{-1} represents a light/heavy rainfall rate threshold, as estimated from R(Zenh). Note that this methodology is very similar to that intended for use under minimally-or-greater terrain-blocked conditions in the targeted, WSR-88D Dual-Polar QPE algorithm, in situations where the hydrometeor type *is* heavy rain or rain-hail mix.

We found that the overall effect of introducing Kdp estimates into the rainrate calculations was to sharply decrease rainrates in cases with high horizontal reflectivity, and to increase rainrates in cases with low-to-moderate reflectivity. As shown in Fig. 2a, the average R(Kdp) rainfall at points with R(Z90) 1-h rainfall $\geq$ 10 mm h-1 was significantly lower. Conversely, the R(Kdp) rainfall in general was slightly higher than R(Z90) (Fig. 2b). Note that here, we did not have hydrometeor classification available.

3e. QPE Verification data

For our verification fields, we utilized "Stage IV" (Lin and Mitchell 2005) mosaicked, gauge-radar accumulation grids generated from the Multisensor Precipitation Estimator application at the Missouri Basin River Forecast Center (MBRFC) and mosaicked at the National Centers for Environmental Prediction (NCEP). In the region of our study, the WSR-88D radar input to the Stage IV product was primarily from the WSR-88D unit at Denver International Airport (KFTG), which has a virtually unobstructed view of the S-Pol coverage area from the east. These verification fields were prepared on the section of the HRAP grid system, locally centered on the S-Pol radar location. Finally, we translated the accumulation fields determined from the four algorithms from the S-Pol grid to the same, HRAP grid system, in preparation for performing our statistical verification analysis. The panels of Figure 3 show examples of accumulations determined by each of these QPE methods (Fig. 3 a-d), as well as the Stage IV verification field (Fig. 3e), for the 1-h period ending 0000 UTC, 4 July, 2006. Note that precipitation artifacts caused only by terrain blockage but not validated by observed precipitation, such as in a N-S aligned area seen west-to-northwest of the radar in Fig. 3a, b & d, were eliminated in a manual quality control procedure performed prior to the statistical analysis that follows.

4. ANALYSIS

4a. Statistical evaluation stratified according to beam blockage

We performed various statistical analyses comparing the hourly accumulations determined from each of the four QPE methodologies to the Stage IV verification data on the HRAP grid. Statistical fields determined included rainfall ratio, correlation coefficient, and error standard deviation. The criterion for including a given grid box for

a given hour in the analysis was that one among the measures from S-Pol or Stage IV had to be non-zero. All QPE values were determined from elevation 0.5^0; 48,428 samples (i.e. HRAP boxes experiencing precipitation during an individual clock-hour, by our criterion), were included. These samples were distributed over 161 hours during the full experimental period, June-August, 2006. Figure 4 shows the total accumulations over the 161 hours for the four QPE methods (Fig. 4 a-d), and for Stage IV (Fig. 4e). The greatest total accumulations are found to the south-southeast of the radar, in a WSW-ESE running band that spans the partially-blocked sectors depicted in Fig 1b, ranging from 1% to 90%. The broad sector from NNE to ESE of the radar with essentially no blockage (<1%) generally has lesser accumulations, especially at the far range of the radar coverage, to the east. Among the QPE methodologies, R(Z90) and R(n-Kdp) – panels b & c, respectively – have the higher accumulations and are closer to the Stage IV verification field. That verification field (Fig. 4e) reveals a feature of very high accumulations at the farthest range from the radar to the S-SE that is not seen in any of the S-Pol QPE methods. Note that this feature corresponds to the 50-75% blockage regime, as will be discussed below.

Figures 5-8 show the results of these statistical analyses in the form of bar charts, stratified by percentage of beam blockage into four groupings: 0-25%; 25-50%; 50-75%; and 75-90%, as well as all the blockage categories combined (right-hand side). Each percentage category has at least 4,100 members. The figures depict the statistics for average precipitation amounts (in terms of average-areal and average-hourly, respectively): QPE/Stage IV Ratios; Correlation Coefficients; and Error Standard Deviations, respectively.

We first analyzed mean non-zero hourly precipitation and mean areal precipitation totals over the entire 161-h study period. In Fig. 5a, it is seen that when all blockage categories were aggregated together (right-hand side), the mean precipitation estimates from each of the methodologies were less than the Stage IV verification field. When stratified by blockage, the same was true except for a few instances: R(n-Kdp) slightly exceeded Stage IV when blockage < 50%; likewise did R(Z90) in the blockage category 75-90%. Both R(Z90) and R(n-Kdp) provided higher, average estimates than the other two methods. One tendency of note is that the estimates by all methods decrease relative to Stage IV once blockage exceeds 50% (with the exception of R(Z90) in the 75-90% blockage grouping). This is true even for the methodologies R(n-Kdp) and R(Kdp-h) that are dependent – fully or partially – on the specific differential phase field. Another tendency observed is that, for all the S-Pol methodologies (except R(Z0)) and the Stage IV field, the areal mean precipitation over the entire experimental period increases as a function of increased blockage and – by inference – higher terrain.

Average hourly totals (Fig. 5b) account for all cases in which at least one of the S-Pol or Stage IV estimates was non-zero. It is seen that for all the S-Pol methodologies and, to a slight extent the Stage IV field, the average hourly precipitation intensity decreases as a function of increased blockage – the opposite tendency as observed for the areal mean, or storm total precipitation. We thus infer that there were more raining hours, and greater

seasonal totals, though lighter average hourly rates, in the mountainous Front Range area than in the plains to the east.

When these data are displayed as S-Pol to Stage IV ratios, underestimation by R(Z) in blocked areas is apparent (Fig. 6). We also note that the R(n-Kdp) and R(Kdp-h) still appear to have a low bias in the higher blockage categories.

Analysis of all individual hourly precipitation amounts in the dataset confirms that all of the QPE estimates had a negative correlation relative to per cent beam blockage. This correlation was very small for Stage IV and R(Z90), namely -0.02 and -0.04 respectively. The correlations for R(Z), R(n-Kdp), and R(Kdp-h) were -0.13, -0.09, and -0.07, as might be inferred from Fig. 5b. Also, the correlations of the S-Pol / Stage IV ratios to beam blockage were -0.27, +0.03, -0.09, and -0.02, for R(Z), R(Z90), R(n-Kdp), and R(Kdp-h), as suggested by Fig. 6. This analysis confirms that the Kdp-based estimates in our study are affected by beam blockage – more so than the corrected R(Z90) fields, though less so than the uncorrected R(Z) estimates.

Figure 7 illustrates S-Pol to Stage-IV correlation in two ways, namely in terms of the spatial pattern of long-term total rainfall (Fig. 7a) and in terms of hourly amounts distributed across all areas and events (Fig. 7b). We infer that all of the S-Pol estimates represent the spatial pattern of rainfall within each blockage category about equally well; however in considering the complete spatial pattern, the low bias that characterizes R(Z) in partially blocked sectors leads to its markedly lower correlation (the 'All' category in Fig. 7a). For correlation relative to hourly rainfall in general, Fig. 7b indicates that all the S-Pol estimates have fairly similar correlation characteristics, with R(Z90) and R(Kdp-h) – which are fully or partially dependent on the traditional Z-R relationship – slightly outperforming the others in the overall category, and R(n-Kdp) showing a slightly lower correlation. The correlations of all the estimators dropped in the 50-75% blockage category, with those dependent on Kdp doing so at about the same rate as the others. Interestingly, all the estimators largely recover in the 75-90% grouping. This we relate to the earlier finding (see Fig. 4) of a local maximum in the Stage IV field (Fig 4e) at the far ranges to the S-SE of the radar, coincident with the 50-75% blockage category, that was not, likewise, seen in any of the rainfall estimation methodologies. This, we infer, resulted in underestimates, and lower statistical correlations, for all the estimation methodologies in the 50-75% category.

It appears that even in the presence of considerable beam blockage, the uncorrected horizontal reflectivity R(Z) still retains considerable information, in that the correlation coefficient for R(Z) is nearly as high in the 75-90% category as it is in the 0-25% category (0.81 and 0.86, respectively). This is consistent with the result that the blockage-adjusted R(Z90) had a very high correlation to Stage-IV overall.

Similar results were obtained from the S-Pol to Stage-IV error standard deviation analysis (Fig. 8), which provides an estimate of the magnitude of random errors that cannot be corrected by simple bias adjustment. As shown in Fig. 8a,b, the estimators dependent only on Z generally have the higher error standard deviations, and as in the previous

analyses, all the estimators – including R(n-Kdp) – perform most poorly in the 50-75% blockage category.

4b. Assessment

From an across-the-board perspective of all the above statistics, we find that the R(n-Kdp) estimator might well be affected by the presence of partial beam blockage, with its performance generally declining as a function of increasing beam blockage to a similar degree as our other estimators. Meanwhile, we get fairly good performance by correcting the traditional Z-R relationship to a higher percentage of blockage, 90%, than is normally accepted in operational practice, 50%. In a head-to-head comparison, the R(Z90) estimator performs about similarly to, if not slightly better than, the R(n-Kdp) estimator. Overall, R(Z90) provides slightly higher correlations while R(n-Kdp) provides lower random errors; however, in the 50-75% percentile-grouping, R(Z90) slightly outperforms R(n-Kdp) in both correlation and random error. Our estimator that performs best, overall – the "hybrid" methodology, R(Kdp-h) – is the one most analogous to that employed in the targeted, operational, WSR-88D Dual Polar QPE algorithm in conditions of heavy rain or rain-hail mix.

5. SUMMARY AND CONCLUSIONS

The results from our Colorado S-Pol experiment indicate that unenhanced precipitation amounts derived from horizontal polarization were substantially underestimated in areas of large beam blockage, as might be expected. However, augmenting the returned, base reflectivity power proportionally to the amount of blockage yielded fairly reliable estimates, even in sectors with significant blockage (up to 90%). This finding suggests that, within any one local sector affected by terrain blockage within some limited percentage interval, the time history of precipitation can be reliably retrieved from uncorrected Zh, though the blockage introduces a low bias in the resulting estimated rainfall spatial field.

Our estimates based primarily on Kdp, particularly our R(n-Kdp) field, become biased low in areas of partial beam blockage, suggesting sensitivity to terrain blockage. This finding is in contrast to prevalent thinking regarding the behavior of Kdp as a precip estimator. It is possible that this result was due in part to application of the algorithm to all hydrometeor types; current plans are to use R(Kdp) operationally (in the WSR-88D algorithm) only in heavy rain or rain/hail situations. It is also potentially significant that some studies indicating Kdp is insensitive to beam blockage were based on C-band, rather than S-band, radar (Friedrich et al. 2007). Signal to noise ratios for Doppler moments are generally higher at wavelengths shorter than S-band, which enables more reliable retrieval of Kdp in light rainfall (Matrosov et al. 2006) and possibly in situations with terrain occultation.

The estimator that performed the best in terms of correlation coefficient and error standard deviation, R(Kdp-h), is essentially similar to that employed in the WSR-88D

Dual Polar QPE algorithm in situations of non-zero partial beam blockage. This is encouraging, in light of the fact that the DPQPE algorithm is intended for national, operational implementation.

These findings could have some practical implications, since the current operational practice for the WSR 88D precipitation processing system is to ignore reflectivity data collected wherever beam blockage exceeds 50%. For such locations, reflectivity from the next higher, unblocked antenna elevation is used instead, even though the radar might overshoot some precipitation at the higher altitude, thus providing an estimate less indicative of what is actually occurring at the ground.

The results shown here might be specific to the summer precipitation environment of the Colorado Front Range and high plains area, which is primarily convective. It is also possible that in cooler situations, with shallower precipitating clouds, beam blockage effects would be more pronounced, and power augmentation might not sufficiently correct Z-R precipitation estimates. Finally, the S-pol unit features some fundamental differences relative to the proposed WSR-88D dual-polarization design, such as a mechanical polarization switch vs. simultaneous vertical/horizontal transmission (NCAR 2010; NSSL 2008). We have not attempted to speculate on the influence of these radar differences in extending these findings to the WSR-88D.

Still, our results indicate that further investigation is warranted to determine if the blockage limitation on precipitation estimates determined from the Z-R relationship should be extended to a higher percentage; based on our results, we would suggest perhaps as much as 75%.

6. ACKNOWLEDGEMENTS

We are indebted to staff of the NCAR Earth Observing Laboratory, particularly Scott Ellis and John Hubbert, for assistance in interpreting the S-Pol data used in the execution of these tasks.

Stage IV precipitation data is prepared at NWS River Forecast Centers, geographically composited in the NWS National Precipitation Verification Unit at NCEP. We retrieved the data from archives maintained by the NCAR Earth Observing Laboratory.

Ron Guenther, NWS Office of Operational System Radar Operations Center, provided the beam blockage estimates for the Oregon and Colorado S-Pol sites.

Work on mitigation of radar partial beam blockage was supported by the National Weather Service Radar Operations Center. Work on radar coverage patterns was supported by the NWS Advanced Hydrologic Prediction Service initiative.

7. REFERENCES

Brandes E.A., 2000: Dual-polarization radar fundamentals and algorithm prospects, Report on Next Generation Weather Radar Program – Operational Support Facility, WSR-88D Commerce-Defense-Transportation, May 2000.

Friedrich, K., Germann, U., Gourley, J., Tabary, P., 2007: Effects of Radar Beam Shielding on Rainfall Estimation for the Polarimetric C-band Radar. *J Atmos. and Ocean. Tech*., **24**, 1839-1859.

Filiaggi, M., S. Smith, M. Churma, L. Xin, and M. Glaudemans 2002: Flash flood monitoring and prediction Version 2.0: Continued AWIPS modernization. *Preprints, Interactive Symposium on the Advanced Weather Interactive Processing System (AWIPS)*, Orlando, Amer. Meteor. Soc., J179-J182.

Fulton, R., J. Breidenbach, D.-J. Seo, D. Miller, and T. O'Bannon, 1998: The WSR-88D rainfall algorithm. *Wea. Forecasting*, 13, p377–395. .

Lin, Y., Mitchell, K.E., 2005. The NCEP Stage II/IV hourly precipitation analyses: Development and applications. *Preprints, 19th Conference on Hydrology.* San Diego, Amer. Meteor. Soc., **1.2**.

Lang, T. J., S. W. Nesbitt, and L. D. Carey, 2009: On the correction of partial beam blockage in polarimetric radar data. *J Atmos. and Ocean. Tech*., **26**, 943-957.

Matrosov, S. Y., and Coauthors, 2006: A comparative study of rainfall retrievals based on specific differential phase shifts at X- and S-Band radar frequencies. *J. Atmos. Oceanic Technol.,* **23**, 952-963.

National Center for Atmospheric Research, 2010: S-pol. [http://www.eol.ucar.edu/instrumentation/remote-sensing/s-pol]

National Severe Storms Laboratory, 2008: Polarimetric Doppler Radar. [http://www.nssl.noaa.gov/divisions/radar/dualpol/].

Park, H.-K., A. Ryzhkov, D. Zrnić, and K.-E. Kim, 2009: The Hydrometeor Classification Algorithm for the polarimetric WSR-88D: Description and application to an MCS. *Wea. Forecasting*, **24**, 730-748.

Reed, S.M., and D.R. Maidment. 1999. Coordinate transformations for using NEXRAD data in GIS-based hydrologic modeling. *Journal of Hydrologic Engineering*, **4**,174-182.

Roberts, R.D., F. Fabry, P.C. Kennedy, E. Nelson, J.W. Wilson, N. Rehak, J. Fritz, V. Chandrasekar, J. Braun, J. Sun, S. Ellis, S. Reising, T. Crum, L. Mooney, R. Palmer, T. Weckwerth, and S. Padmanabhan, 2008: REFRACTT 2006. *Bull. Amer. Meteor. Soc.*, **89**, 1535–1548.

Ryzhkov, A., S. Giangrande, and T. Schuur, 2005a: Rainfall Estimation with a Polarimetric Prototype of WSR-88D. *J. of Appl. Meteor.*, Vol. **44**, No. 4, pp. 502—515.

_____, Schuur, T., Burgess, D., Heinselman, P., Giangrande, S, and Zrnic, D., 2005b: The Joint Polarization Experiment: Polarimetric Rainfall Measurements and Hydrometeor Classification. *Bull. Amer. Meteor. Soc*. **86**, 809-824.

Smith, M.B., Seo, D.-J., Koren, V.I., Reed, S., Zhang, Z., Duan, Q.-Y., Cong, S., Moreda, F., Anderson, R., 2004b. The distributed model intercomparison project (DMIP): motivation and experiment design. *J. Hydrology*, 298(1-4), 4-26.

Smith, S. B., J. Roe, M. T. Filiaggi, M. Glaudemans, M. E. Churma, L. Xin, and R. Erb, 2000: Flash flood monitoring and prediction in AWIPS Build 5 and beyond. *Preprints, 15th Conf. on Hydrology*, Long Beach, Amer. Meteor. Soc., 229-232.

Zrnic, D., Ryzhkov, A., 1996: Advantages of Rain Measurements Using Specific Differential Phase. *J. Atmos and Ocean Tech*., **13**, 454-463.

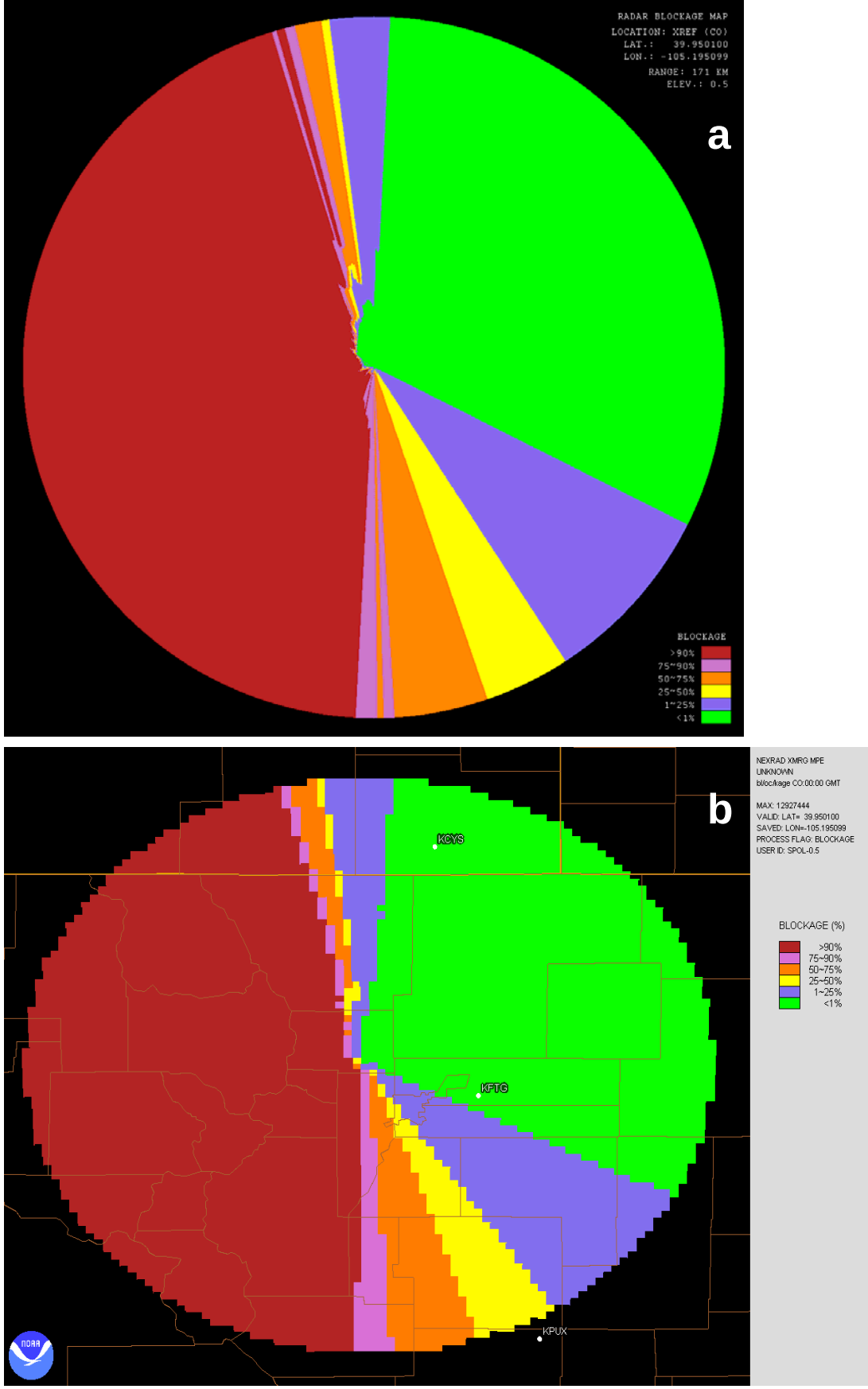

Figure 1. **Beam blockage** at 0.5^0 for Colorado on (a) S-Pol grid centered at S-Pol site east of Boulder, and (b) in HRAP projection

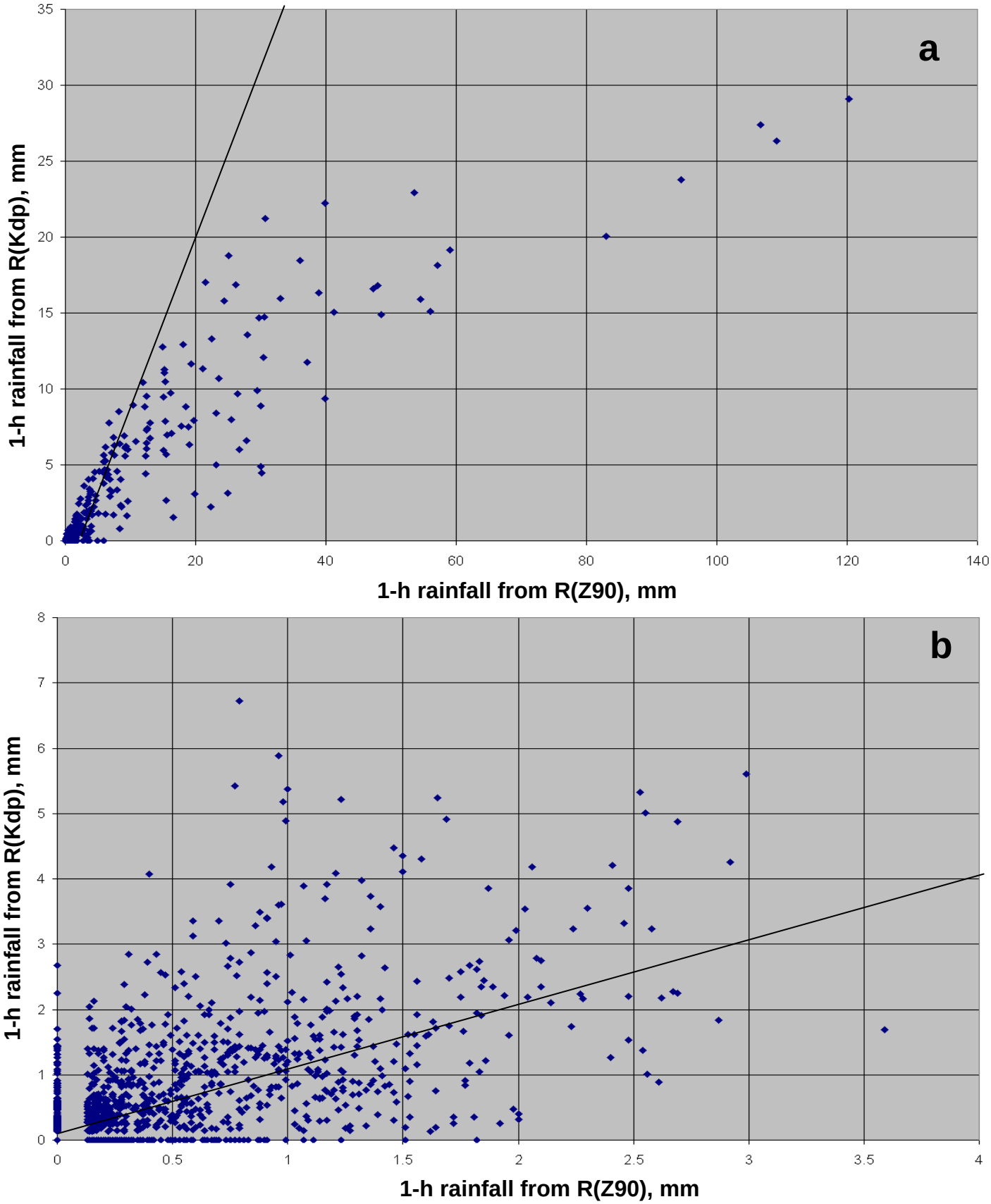

Fig 2a: Correlation between R(Kdp) (vertical axis) and R(Z90) (horizontal axis) in (a) heavy rain (>10.0 mm/hr, as determined by R(Z90) method), and (b) lighter rain.

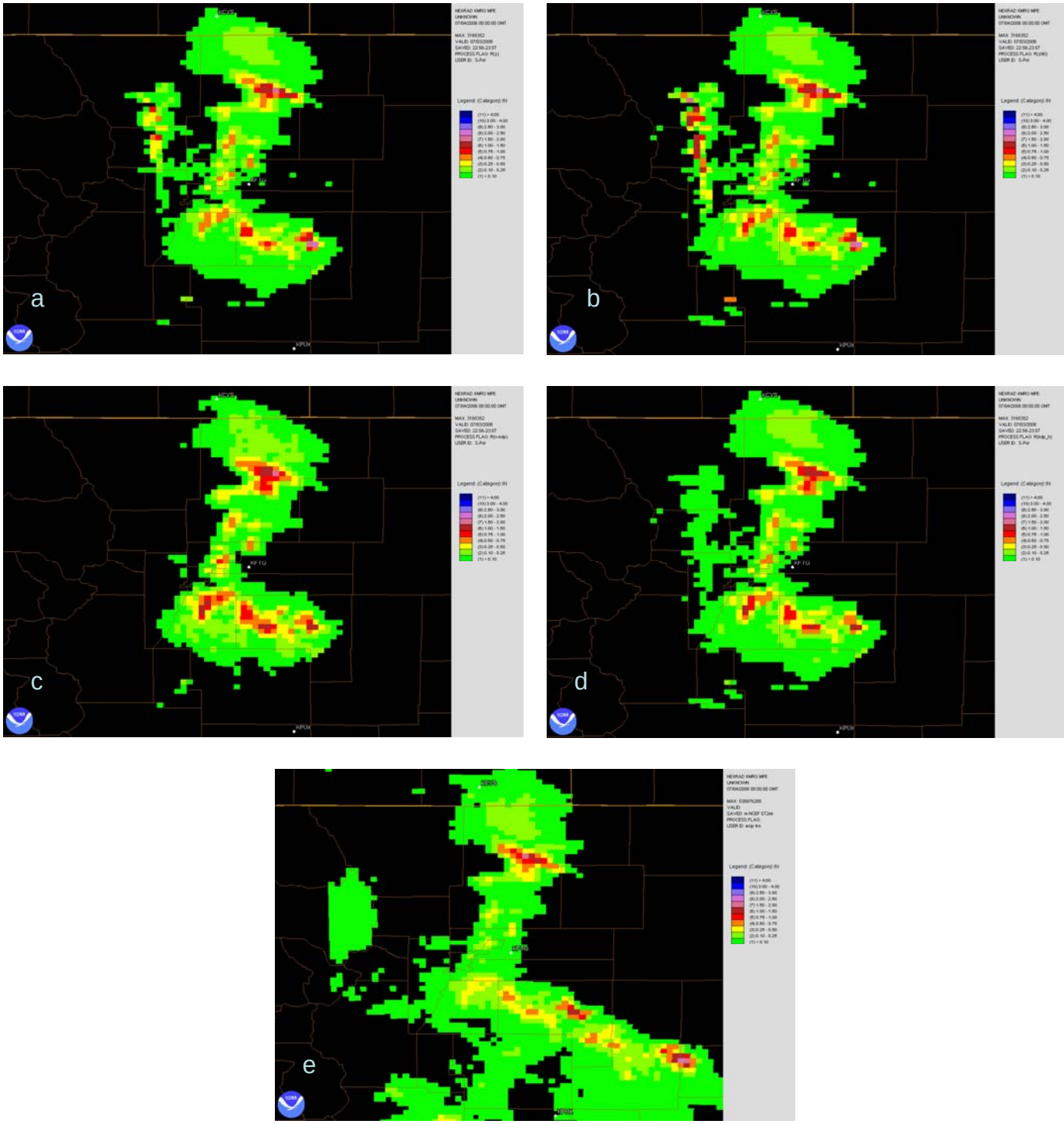

Figure 3. **1-hour accumulations** at 0.5^0 for Colorado on ~4x4 km^2 HRAP grid centered at S-Pol site east of Boulder, **ending 07/04/2006, 00z**: a) $R(Z_0)$; b) $R(Z_{90})$; c) $R(n\text{-}k_{dp})$; d) $R(K_{dp}\text{-}h)$*;* also e) Stage IV (verification).

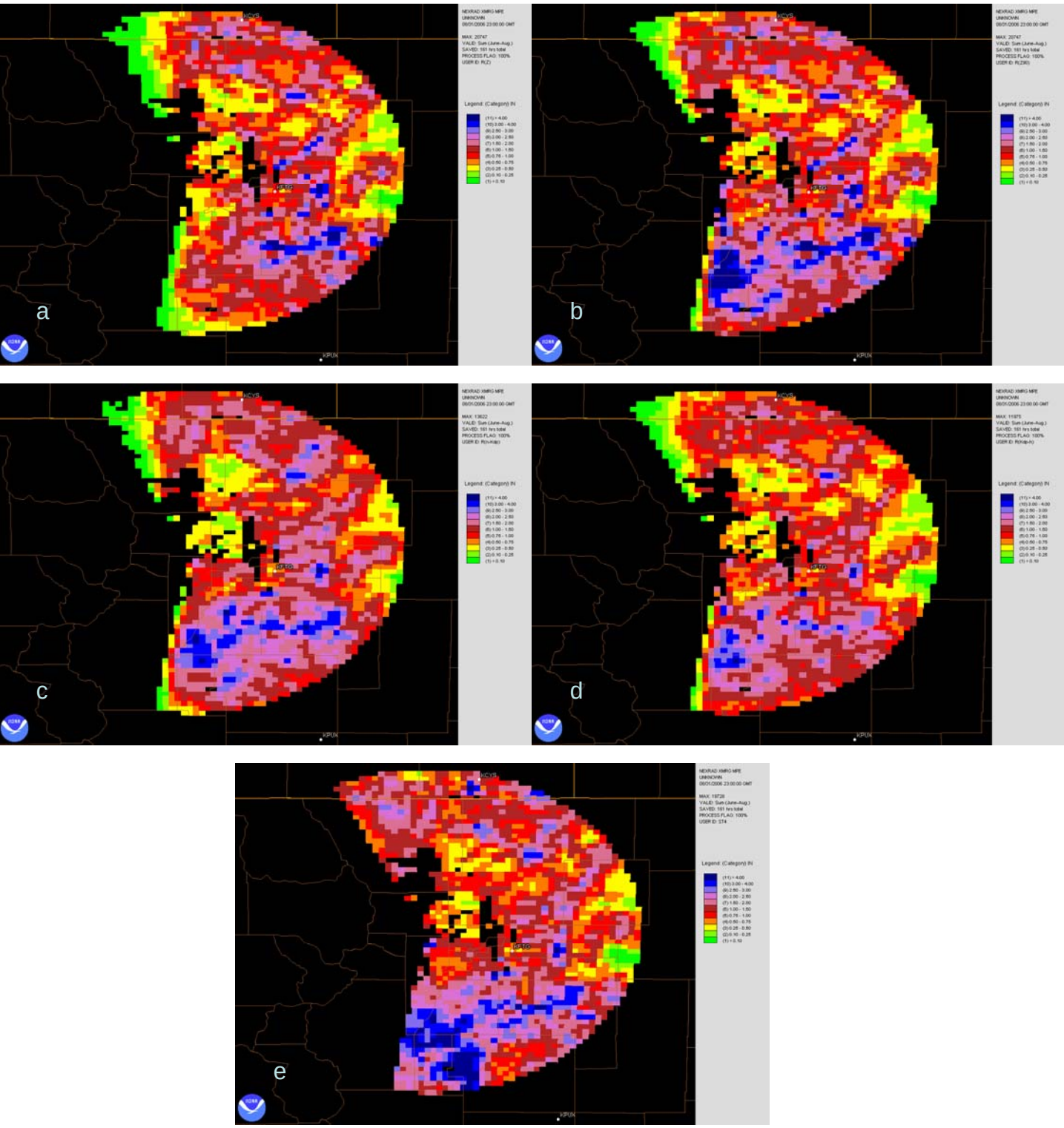

Figure 4. Long-term, **summer-season accumulations** (161 hours during June, July, August 2006) at 0.5^0 for Colorado on ~4x4 km^2 HRAP grid centered approx. at the S-Pol site: **a)** $R(Z_0)$; **b)** $R(Z_{90})$; **c)** R(n-kdp); **d)** R(Kdp-h)*;* also **e)** Stage IV (verification). Grid points determined by subjective QC analysis to be substantially contaminated by clutter were removed (appear as background black) and not included in statistical analyses. Note, in comparison to Fig. 1, the general correspondence of the greater accumulations with the higher terrain/partially blocked regions of the Rockies Front Range to the north and south of the radar location, and of the lesser accumulations with the Plains/unblocked regions to the east. The high Rockies to the west of the radar are totally blocked and not included in the analysis.

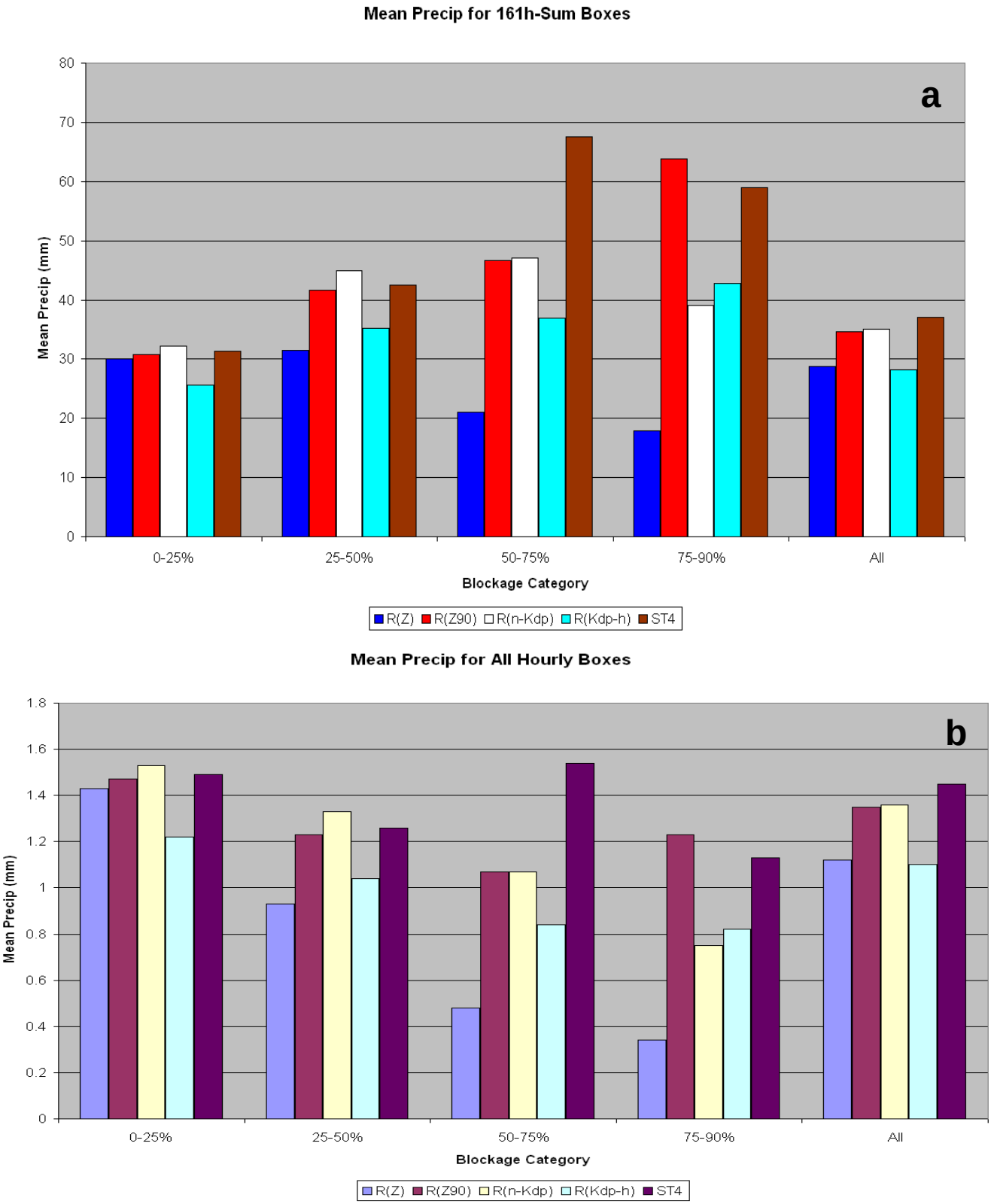

Figure 5. **Average precipitation** as a function of blockage category, by various QPE methodologies (blue: R(Z_0); red: R(Z_{90}); white: R(n-K_{dp}); turquoise: R(K_{dp}-h)) and Stage IV verification (brown or purple). **(a)** Average, areal seasonal totals (0-25% blockage: 30,728 HRAP grid boxes; 25-50%: 5,006 boxes; 50-75%: 8,587 boxes; 75-90%: 4,107 boxes; all cases together: 48,428 boxes); **(b)** average non-zero hourly amounts (0-25%: 1,464 HRAP grid boxes; 25-50%: 148 boxes; 50-75%: 196 boxes; 75-90%: 79 boxes; and all cases together: 1,887 boxes).

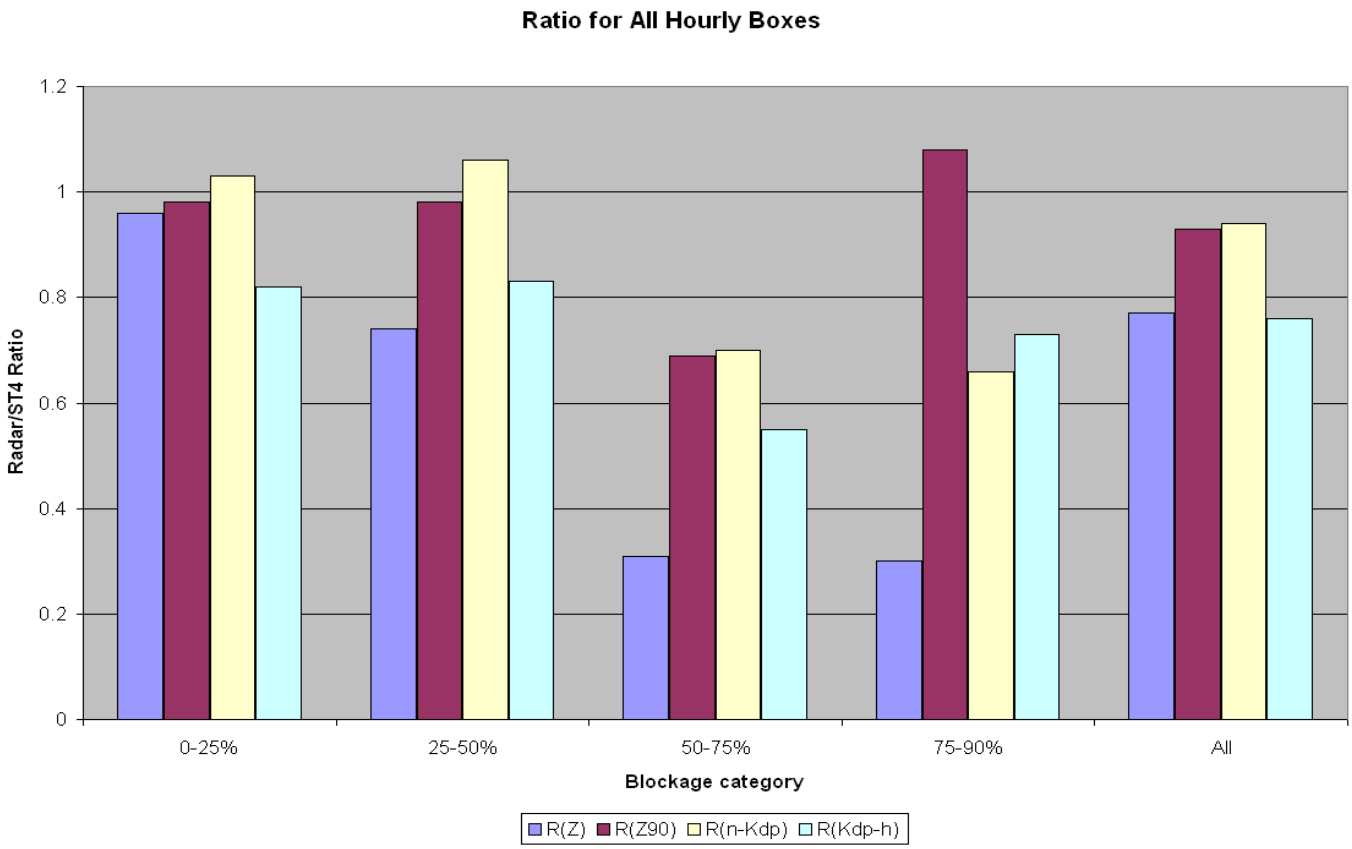

Figure 6. S-Pol to Stage IV **ratios**, stratified by blockage category.

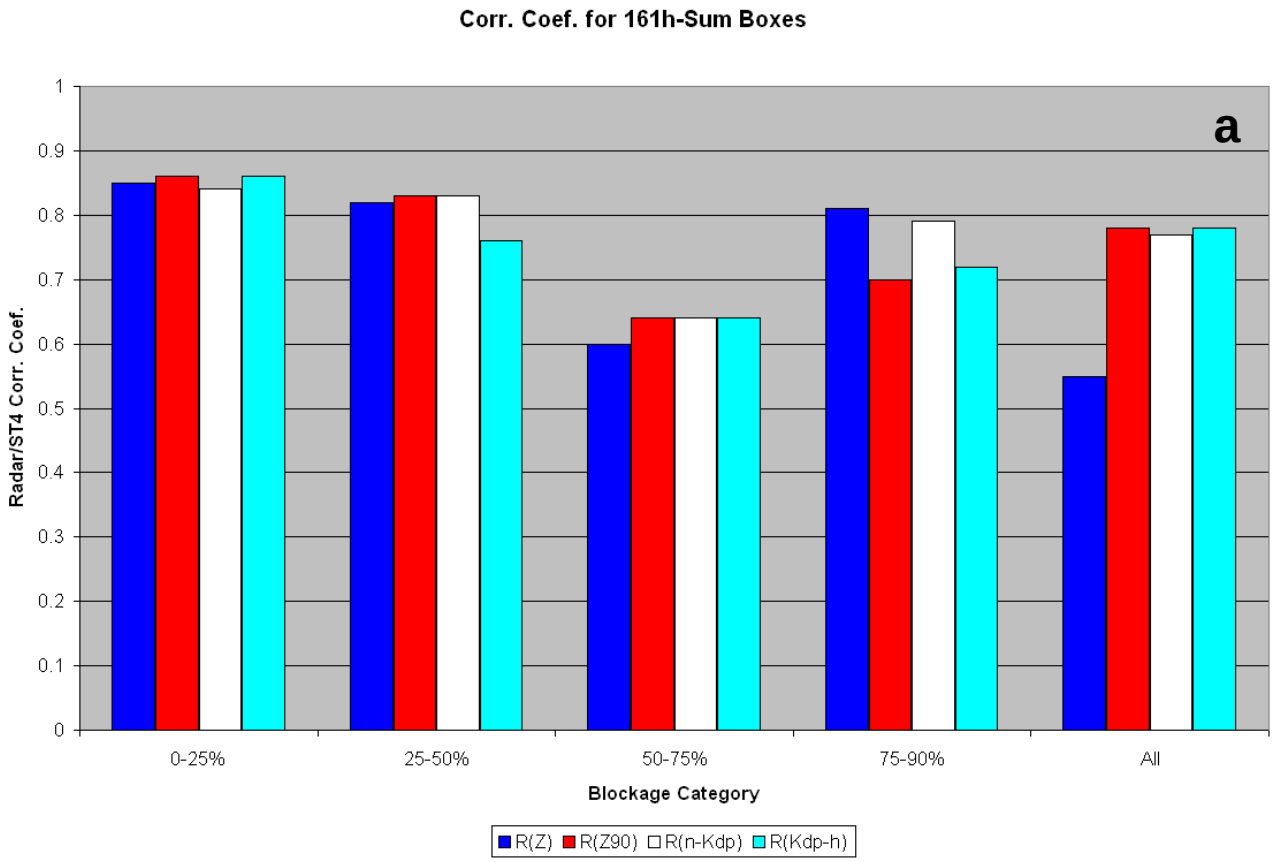

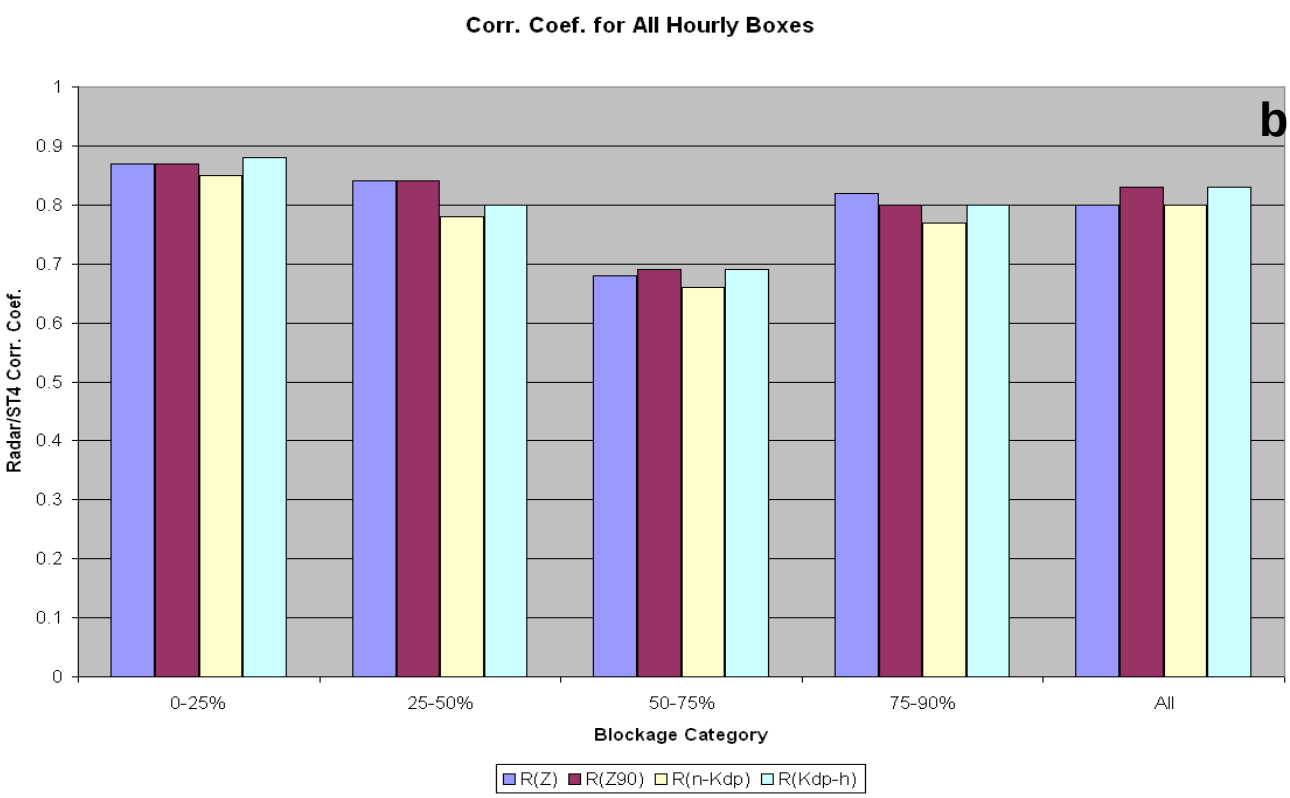

Figure 7. S-Pol to Stage IV **correlation coefficients**, for (a) rainfall total over all 161 h combined, and (b), all nonzero hourly totals considered individually. Correlations in (a) are essentially those for the spatial pattern of total precipitation

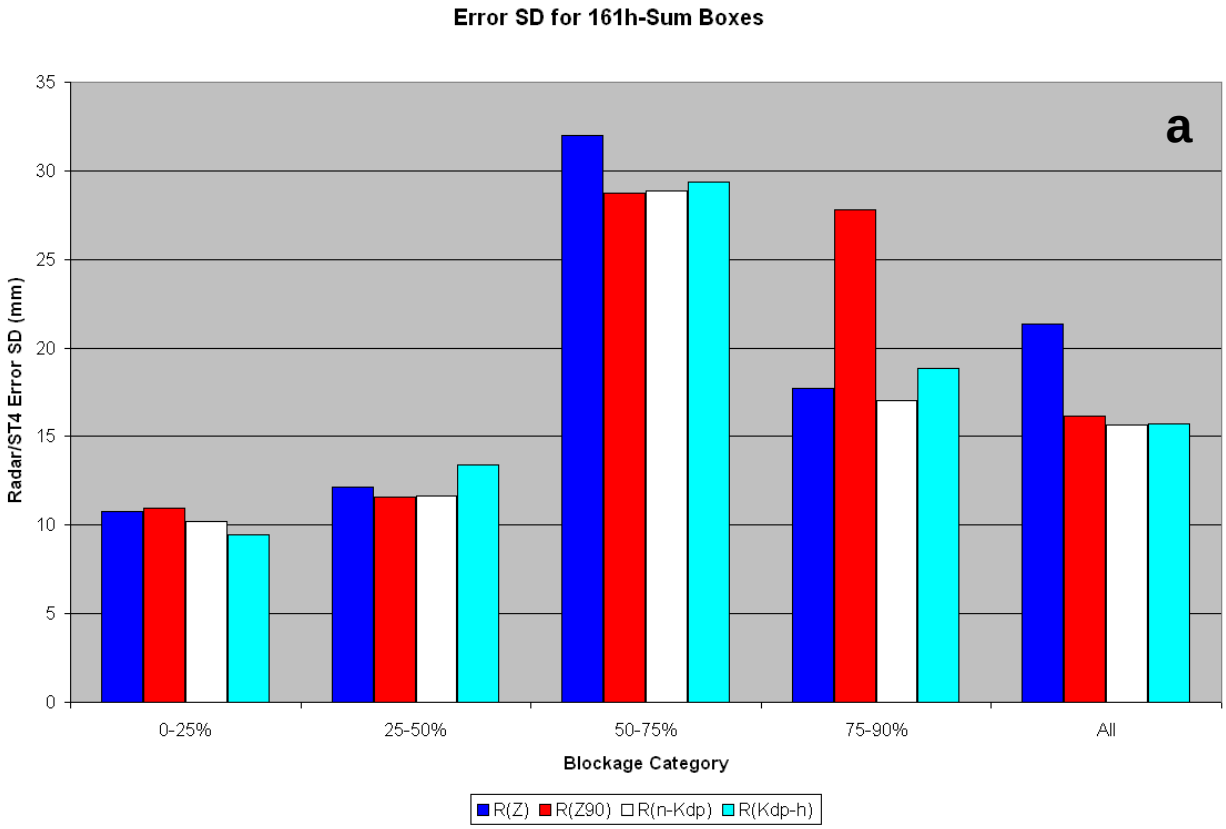

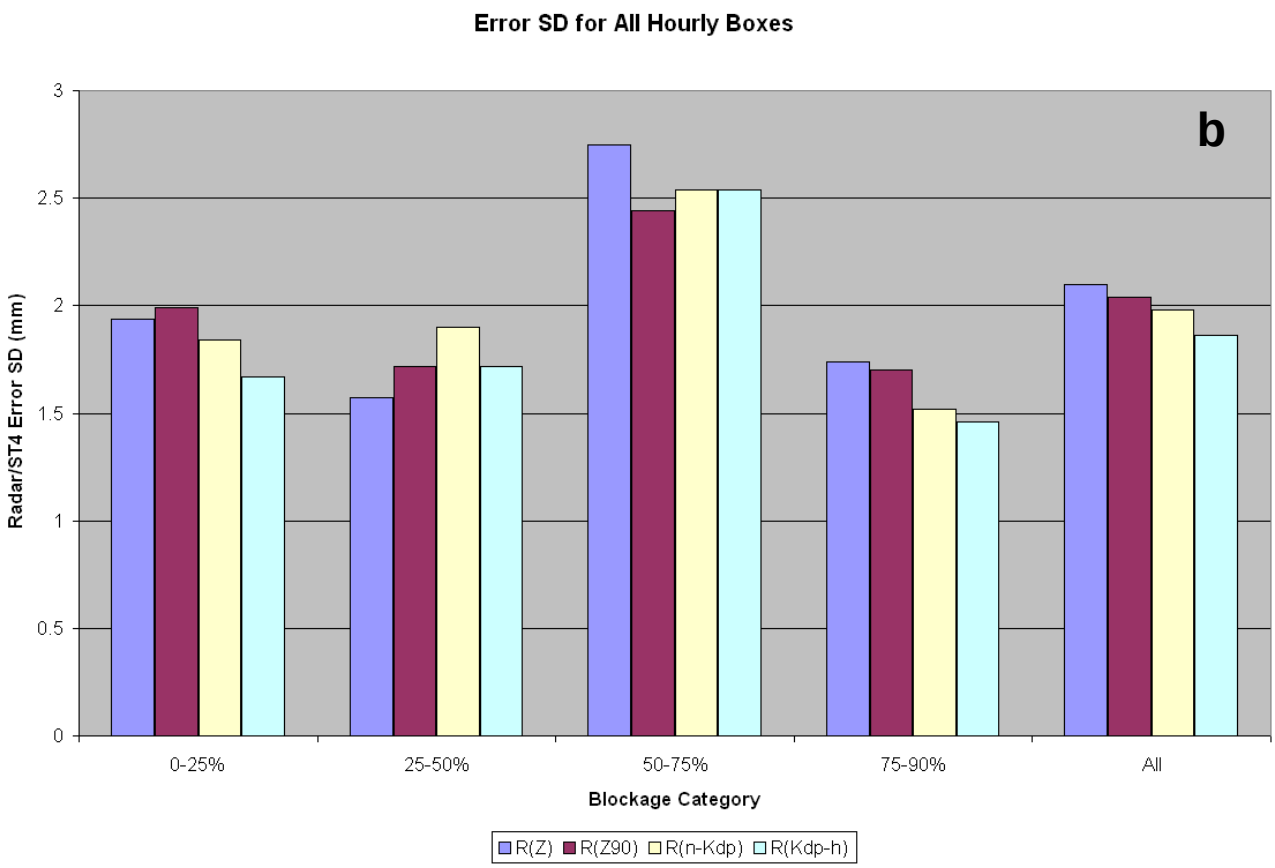

Figure 8. As in Fig. 6, except for **Error Standard Deviation**.

Task 2. Collection of surface snowfall estimates for use in validation and calibration of dual polarimetric radar-based snowfall algorithms

The collection of data in developed under this task was forwarded to ROC and NSSL staff in 2009, and described in the previous MOU report. Work on the task has been suspended until the relevant radar data can be recovered, or radar data collection can be resumed.

Task 3. Investigate modification of MPE bias table to apply to dual pol. QPE

1. Introduction and justification

Spatial and temporal changes in hydrometeor characteristics, beam spreading, vertical reflectivity profile effects, and variations in calibration between radars all necessitate routine bias correction of single-polarization rainfall estimates (eg. Fulton 1999; Johnson et al. 1999; Steiner et al. 1999). An operational system for global (mean-field) and local gauge/radar bias correction was implemented in earlier versions of the Multisensor Precipitation Estimator (MPE) (Seo et al. 1999; Seo and Breidenbach 2002). In this subsystem of AWIPS, hourly gauge rainfall reports are collocated with 1-h radar rainfall estimates from Digital Precipitation Array (DPA; Fulton et al. 1998) products. A gauge/radar bias correction factor is estimated as the ratio of the sums of recent nonzero gauge and nonzero radar estimates. The correction factor is applied to some MPE products, and is transmitted back to the Radar Product Generator (RPG) for inclusion as text information with new DPA products. The bias factor can be applied to precipitation products other than the DPA prior to output, if specified by staff at the controlling the radar unit.

It is expected that dual-polarization QPE (DPQPE) will substantially mitigate the need for bias correction, particularly in cases when all precipitation can be observed below the melting layer. Through the Hydrometeor Classification Algorithm (HCA; Park et al. 2009), dual-polarization moments can indicate the presence of unusual drop-size distributions, detect hail in thunderstorms, and differentiate among rain, melting snow, and dry snow. The DPQPE algorithm package includes adaptations for surface precipitation estimation in conditions where snow is indicated. The initial concept of operations for dual-polarization radar did not include bias correction factors as product information.

However, there is still uncertainty on the interpretation of the suite of dual-polarization moments, in terms of rainfall or precipitation rate. For instance, estimation of surface rainfall is complicated in cold situations, in which the radar can sometimes detect only dry or melting snow more that at ranges more than a few tens of km from the radar. The range of sizes and shapes of snow crystals render interpretation of liquid water content below the melting layer very uncertain. Current plans involve estimation of vertical profiles of reflectivity and other moments to at least partially correct for these factors, but the success of this approach is not guaranteed.

The need for routine bias correction will still exist. There is a need to minimize inter-radar QPE differences, due to differences in calibration and operating frequency that cannot be modeled by theory. Also, the MPE package will continue to ingest single-polarization QPE products, such as those from Terminal Doppler Weather Radar, Air Route Surveillance Radar, and possibly products from foreign radar systems.

Moreover, the current bias correction information made available along with operational radar products, a table of time-dependent mean-field bias factors, is of limited utility. The gauge/radar ratio generally increases with range, due to beam overshooting of precipitation and/or detection of snow, which typically yields a larger surface rainfall rate for a given reflectivity factor than does liquid.

Accordingly, we have undertaken an investigation of alternative possibilities for expressing bias information, including range-dependent bias and two-dimensional bias fields. Such two-dimensional fields are presently calculated within MPE but are not disseminated.

2. Bias options to be tested

These options include the long-term bias (a reference for this study only), current mean-field bias, a range-dependent bias factor (determined as the range-smoothed gauge/radar ratio), and a two-dimensional bias, estimated as the local spatially-smoothed average of bias factors interpolated from neighboring gauge-radar points. These biases can be defined as follows:

Long-term bias (LTB):
The bias over all gauge-radar pairs in the sample, equally weighted regardless of age relative to the current time.

Mean-field bias (MFB):
The average sum of nonzero precipitation from gauges divided by the average sum of precipitation from radar at collocated points with precipitation, subject to some minimum number of reports (typically 10) that are as close as possible to current. A weighting factor is introduced in the averages to give lower weight to observations more than two hours old. The MFB is assumed to apply to any point in the radar umbrella. Mean-field bias is currently calculated in MPE.

Range-dependent bias (RDB)
Similar to MFB, except that the bias factor is estimated only from gauges that are within a given radar range band, relative to the point in question.

Local bias (LB):
Similar to MFB and RDB, except that the bias factor is estimated only from gauges that are within a given distance of the point in question. A form of local bias is currently calculated in MPE.

These bias corrections are illustrated in the schematic figure of the distribution of gauge sites within a radar umbrella, in Fig. 9. The white crossmark in the lower right quadrant is the target for bias correction in this schematic.

All models incorporate criteria on the minimum number of effective gauge-radar pairs that must be included in a reliable bias estimate. A minimum number of observations characteristic of the current meteorological situation must be collected for the bias signal to be detected in the presence of random noise.

The density of the surface rain gauge network and the general character of precipitation coverage are limiting factors on the bias models that can be applied. In areas with few rain gauges and generally spotty convective precipitation, it might be impossible to reliably estimate local bias; in the length of time it takes to accumulate enough G-R pairs to estimate the bias, the meteorological situation and hydrometeor characteristics will change. Our investigation will include observations from multiple radar umbrellas with the greatest possible climatic diversity. As needed, we will artificially thin the network of gauges to represent a sparser distribution.

3. Performance metrics

Performance of the models will be estimated based on their performance in cross validation, over the available period of record. An error for any one gauge-radar pair is taken to be that after bias is estimated from all other applicable gauge-radar pairs in the sample, up to and including the current time. Data from the gauge site in question will not be used.

Performance metrics will include bias (which might not be completely eliminated); mean absolute error (MAE) and root-mean squared error; and percentage of cases with large percentage errors, > 25% of the verifying gauge value whenever the hourly rainfall is observed or estimated to be at least 10 mm.

4. Data collection and initial results with legacy DPA data

We plan to test DPQPE rainfall estimates as they become available from the KOUN pre-production unit, and from beta-test units scheduled for deployment later in 2010 and in early 2011. Verifying rain gauge data will be collected from operational and available research data sources, including the Oklahoma Climate Survey mesonet, Agricultural Research Service Little Washita and Fort Cobb micronets, and the HADS data stream.

As an initial test, we have calculated the error metrics described above for a 3-year set of gauge-radar pairs from the current precipitation processing system. Radar data are DPA products collected between 2004 and 2006, paired with hourly rainfall reports collected through the HADS (Hydrometeorological Data System). Data from seven WSR-88D umbrellas were tested, as shown in Table 1.

Input gauge-radar pairs were selected through a form of automated quality control, in which only those gauge sites whose reports had a correlation of at least 0.7 relative to the radar estimates. This criterion removes gauges which have long-standing mechanical or reporting problems. In general 75-80% of the available gauge sites are retained by this procedure.

In this test, the RDB was estimated from gauge-radar pairs that had the same range relative to the radar as the point in question, +/- 25 km. The LB was estimated from other pairs within 60 km of the point in question, an influence radius sometimes applied in MPE.

It should be noted that in these tests, we did not stratify results by season, nor attempt to account for changes in Z-R relationship. Such potential refinements are not included in the current MPE.

However, seasonal stratification will be evaluated later in the study, since the spatial character of precipitation changes substantially during the year in many radar umbrellas.

Two sets of error statistics (MAE and percentage of gauge reports with ≥ 25% amount error) are shown in Tables 2-3, respectively. Error statistics generally follow the intuitive pattern, that bias correction is most effective in the umbrellas with a predominance of larger mesoscale systems and stratiform precipitation (KBGM, KMPX for example). The corrections are least effective in umbrellas with low gauge density and sparse precipitation (eg. KIWA, KFTG). The potential for appreciable improvement by using local, rather than mean-field, bias is apparent in some of the sites, in which the LB approach reduced the percentage of large errors by 0.05 or more see (KFFC, KBGM, and KMPX in Table 3).

5. Collection of data from KOUN and initial deployment sites

Collection of DPQPE and legacy single-pol products from the KOUN test site is being carried out by OHD-HSEB staff, and some data has been collected for major precipitation events such as that of 8-9 April 2010. Subject to agreement that the quality of this data is representative of the post-deployment state, we will carry out similar evaluations to test the effects of bias correction on this DPQPE data in the near future.

REFERENCES

Fulton, R., J. Breidenbach, D-J. Seo, D. Miller, and T. O'Bannon, 1998: The WSR-88D rainfall algorithm. *Wea. Forecasting*, **13**, 377-395.

_____, 1999: Sensitivity of WSR-88D rainfall estimates to the rain-rate threshold and rain gauge adjustment: A flash flood case study. *Wea. Forecasting*, **14**, 604-624.

Johnson, D., M. Smith, V. Koren, and B. Finnerty, 1999: Comparing mean areal precipitation estimates from NEXRAD and rain gauge networks. *J. Hydrologic Engineering*, **4**, 117-124.

Seo, D.-J. and J. Breidenbach, 2002: Real-time correction of spatially nonuniform bias in radar rainfall data using rain gauge measurements. *J. Hydrometeor.*, **3**, 93-111.

Seo, D.-J., J. Breidenbach, and E. Johnson, 1999: Real-time estimation of mean field bias in radar rainfall data. *J. Hydrol.*, **223**, 131-147.

Steiner, M., J. Smith, S. Burges, C. Alonso, and R. Darden, 1999: Effect of bias adjustment and rain gauge data quality control on radar rainfall estimation. *Water Resour. Res.*, **35**, 2487-2503.

Table 1. Characteristics of radar umbrellas and results of tests of 4 bias-correction methods applied to horizontal polarization DPA products and 1-h rain gauge reports, for 2004-2006. Statistics are arranged according to increasing number of gauge sites.

WSR-88D	**Site location**	**Number of gauge sites**	**Number of gauge-radar pairs tested**	**Number of observations with ≥ 0.25 inch**
KIWA	Phoenix	66	9537	955 (10%)
KFTG	Denver	66	7624	667 (9%)
KTBW	Tampa Bay	69	30936	7634 (25%)
KMPX	Minneapolis	71	30441	3940 (13%)
KTLX	Oklahoma City	149	46591	8982 (19%)
KBGM	Binghamton	116	80551	8117 (10%)
KFFC	Atlanta	189	71001	13569 (19%)

Table 2. Mean absolute errors (MAE, inch) for four bias correction methods and original uncorrected estimates, for all applicable cases.

WSR-88D	**MAE, LTB**	**MAE, MFB**	**MAE, RDB**	**MAE, LB**	**Original estimate**
KIWA	0.057	0.058	0.056	0.055	0.065
KFTG	0.051	0.051	0.049	0.048	0.054
KTBW	0.091	0.090	0.090	0.088	0.088
KMPX	0.056	0.054	0.050	0.050	0.063
KTLX	0.082	0.076	0.073	0.071	0.087
KBGM	0.049	0.045	0.042	0.040	0.048
KFFC	0.076	0.070	0.067	0.065	0.074

Table 3. Percentage of radar estimates with percentage error ≥ 25%, for all gauge-radar pairs with ≥ 0.25 inch precipitation as indicated by the gauge or the MRF-corrected radar estimate.

WSR-88D	**% errors, LTB**	**% errors, MFB**	**% errors, RDB**	**% errors, LB**	**Original estimate**
KIWA	0.784	0.845	0.835	0.820	0.803
KFTG	0.814	0.843	0.825	0.823	0.778
KTBW	0.713	0.722	0.706	0.696	0.722
KMPX	0.730	0.758	0.717	0.707	0.725
KTLX	0.767	0.773	0.747	0.727	0.762
KBGM	0.730	0.721	0.696	0.654	0.738
KFFC	0.741	0.737	0.711	0.686	0.745

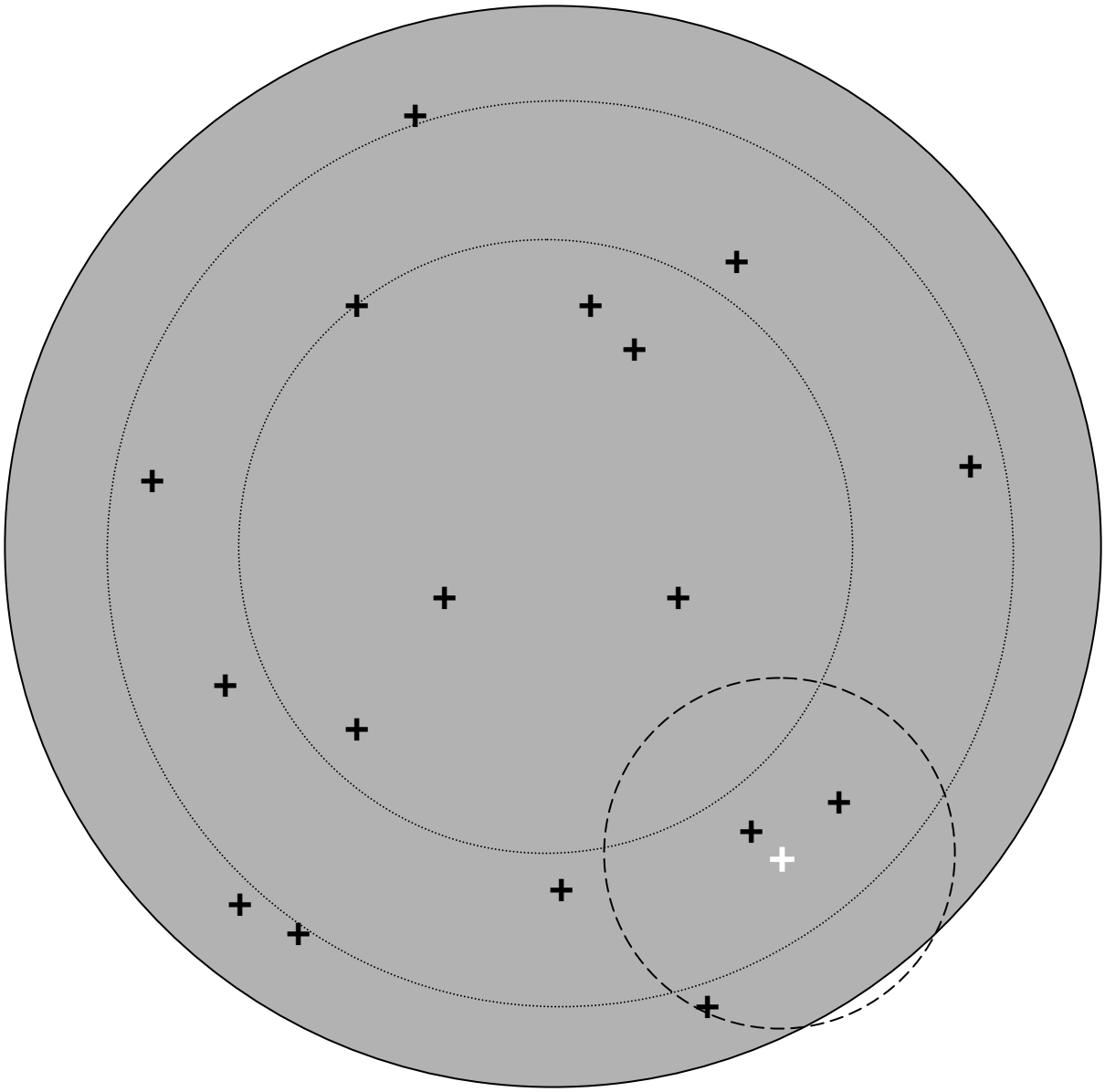

Figure 9. Diagram illustrating search areas for bias corrections at the point indicated by the white cross. Black crosses are other rain gauge locations. All gauges within the shaded circle are used in mean-field and long-term bias estimation; gauges between the dotted circles concentric on the center are used in range dependent bias estimation; gauges within the smaller dashed circle for local bias estimation.